A Single Atomic Particle Forever Floating at Rest in Free Space: New Value for Electron Radius

1988 Phys. Scr. 1988 102

(http://iopscience.iop.org/1402-4896/1988/T22/016)

Physica Scripta. Vol. T22, 102–110, 1988.

A Single Atomic Particle Forever Floating at Rest in Free Space: New Value for Electron Radius

Hans Dehmelt

Department of Physics, University of Washington, 15th Avenue N.E., Seattle, Washington 98195, U.S.A.

Received August 28, 1987; accepted October 7, 1987

Abstract

An updated survey of mostly experimental spectroscopy work in Seattle on an individual closely-confined isolated atomic or elementary particle is presented. The classical notion of an atomic particle at rest in free space is discussed, and shown to be approximable by zero-point confinement of the particle in a laboratory trap. An important tool for cooling the particle, and in the case of an electron, for obtaining directly the difference of spin and cyclotron frequencies ν_s, ν_c, is side band excitation. The quantum numbers of the geonium "atom", an electron in a Penning trap, have been continuously monitored in a non-destructive way by the new "continuous" Stern–Gerlach effect. In this way the g-factors of electron and positron have been determined to unprecedented precision,

$$\tfrac{1}{2}g \equiv \nu_s/\nu_c = 1.001\ 159\ 652\ 188(4),$$

providing the most severe tests of QED and of the CPT symmetry theorem, for charged elementary particles. From the close agreement of experimental and theoretical g-values a new, $10^4 \times$ smaller, value for the electron radius, $R_g < 10^{-20}$ cm, may be extracted. Other important results are: confinement of the individual positron, Priscilla, for 3 months, a tenfold suppression of the natural width of the cyclotron resonance, detection of an isomeric (cyclotron-excited) state via mass-spectroscopy, isolation and continuous detection of an individual proton, confinement of ≈ 100 antiprotons slowed to ≈ 3000 eV, confinement of a Ba^+ ion to ≈ 100 nm, and the demonstration of quantum jumps in geonium and in an isolated, individual regular atomic particle, Ba^+. Some new experiments are proposed.

Daß ich erkenne, was die Welt im Innersten zusammenhält.
GOETHE, "*Faust*"

"(*The scientist*) *appears as* realist *insofar as he seeks to describe a world independent of the acts of perception; as* idealist *insofar as he looks upon the concept and theories as the free inventions of the human spirit (not logically derivable from what is empirically given); as* positivist *insofar as he considers his concepts and theories justified* only *to the extent to which they furnish a logical representation of relations among sensory experiences. He may even appear as* Platonist *or* Pythagorean *insofar as he considers the viewpoint of logical simplicity as an indispensable and effective tool of his research.*"
EINSTEIN

1. Introduction

In this paper I update earlier surveys of a similar nature [1–3], and propose some new experiments. Apologizing to others, I will mostly confine myself to work carried out at the University of Washington.

Figure 1 shows a photograph, taken by my colleague Nagourney in connection with our shelved (optical) electron amplifier experiments [5]. The small (*blue*) dot in the center is barium ion Astrid, whom we provided with an identity in the lime light lasting some 6 hr. Thus, there must be some *reality* to my title, A Single Atomic Particle Forever Floating at Rest in Free Space (SAPARIS for short) [2, 6]. The photograph also graphically demonstrates the soundness of my 1956 claim [7]: Ions in a trap are promising objects for high-resolution spectroscopy. As an example of trapping schemes [1] demonstrated by then, I mentioned the purely electrostatic trap of Kingdon [8]. It ante-dates Lawrence's cyclotron trap [9], and is free from variable Zeeman-shifts. I followed up my 1956 claim in the same year with the first spin resonance experiments on $\approx 10^{11}$ free electrons confined in a space charge trap, whose number was monitored by their damping of an 25 MHz LC circuit, and demonstrated a Penning trap in 1959 [6]. Together with Major in 1962 I reported similar experiments on $\approx 10^7$ He^+ ions [6] in a Paul trap.

The SAPARIS concept is obviously a classical idealization, related to the basic mathematical abstraction of a point in space. It takes reductionist atomism to the limit. In addition, an isolated individual material point particle at rest in space is the starting point of classical mechanics, and an elementary Dirac particle, such as the electron, is the closest laboratory approximation of a point particle. My interest was aroused, when my teacher Richard Becker drew a dot on the blackboard declaring "Here is an electron . . . ". Minding Heisenberg's admonition, to focus on observables, and knowing about ion traps in radio tubes, I began to wonder, how to duplicate Becker's localization feat in the laboratory. I discussed detection of the signal [1, 6, 10], and also zero-point confinement [6] of a mono-ion oscillator early on, and the first mono-electron oscillator *experiment* was carried out at the University of Washington by Wineland *et al.* [11].

Even for an anti-hydrogen atom floating at rest in the inertial frame of a satellite lab [3], the closest quantum-mechanical approximation of the concept appears to be the confinement in the *zero-point* level of a laboratory well, see

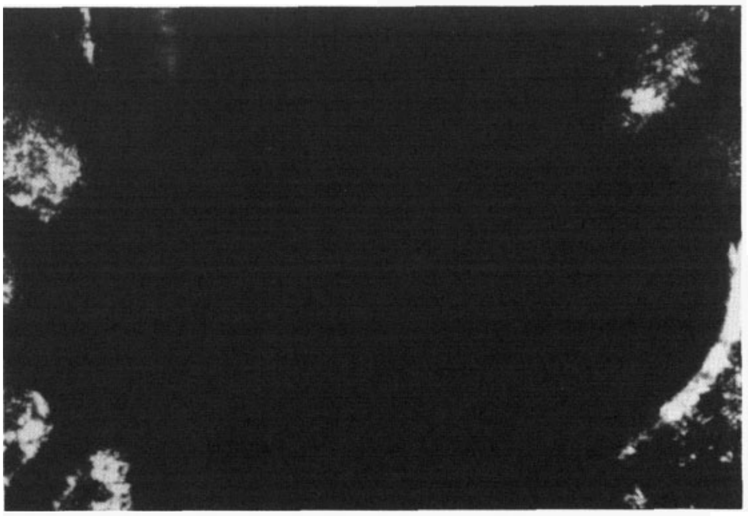

Fig. 1. Photograph of individual (blue) Barium ion Astrid. Stray light from the lasers illuminates the 0.7-mm internal diameter ring electrode of the tiny r.f. trap. A colour reproduction can be found on a separate page. An individual isolated atom was first photographed in Heidelberg [4].

Fig. 2. Steering the satellite so as to keep the atom more or less in the center of the confining box would minimally require sensing the position of the atom, when it approaches the wall, to even closer tolerance than the dimension of the box, thereby introducing an even larger uncertainty in the particle momentum. For a box size of $\frac{1}{2}$ mm the zero-point velocity is ≈ 0.4 mm/s [6], equivalent to a temperature $\approx 10^{-11}$ K. Soft non-material walls for a "box" could easily be provided by a magnetic trap of the type recently demonstrated by H. Hess *et al.* [12], employing fields no larger than 10^{-4} Gauss. "Free space", of course, can only be approximated: one must carefully minimize all undesired fields and couplings at the particle site, including trapping fields. Thanks to modern cryogenic techniques the attainment of a perfect vacuum free of residual gas seems to be the least of the problems here.

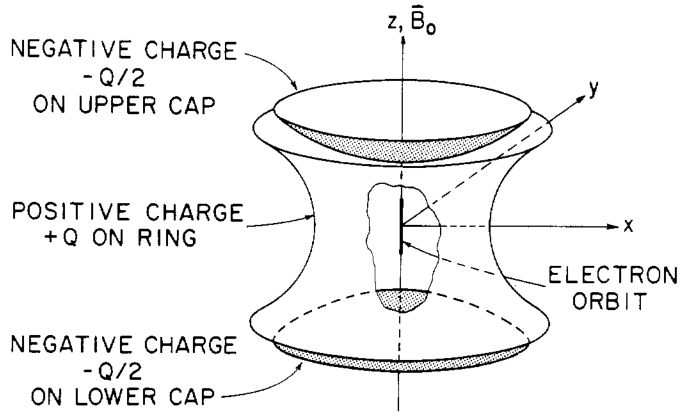

Fig. 3. Geonium atom. The atom consists of an individual electron in the center of a Penning trap [1, 14]. The trap design is related to that of the widely used Penning discharge. The E-field is 0 in the center.

2. Example of zero-point confinement: geonium

Such extreme confinement so far has been realized, by Van Dyck *et al.* [13], at liquid helium temperatures, only for the 150 GHz cyclotron motion of geonium, Fig. 3, an electron in a Penning trap [1, 6, 14]. Figure 4 shows the energy levels of this metastable pseudoatom [15, 16]. Here, radiation damping quickly causes the cyclotron radius to shrink to its zero-point value

$$\langle r_c^2 \rangle_{00} \approx (100\,\text{Å})^2.$$

How do we know this? Our *continuous* Stern–Gerlach effect *experiment* on an electron in a classical orbit does work, in spite of Pauli's now obviously erroneous general edict (a new Pauli "Verbot") stating the opposite, which was published in 1932 and set off a still persisting wave of quantum-mystification in the literature [17]. Our new experiment makes it possible to actually watch [15, 18] quantum jumps [19, 20] to and from spin states $m = -\frac{1}{2} \leftrightarrow +\frac{1}{2}$, and cyclotron levels $n = 0 \leftrightarrow 1 \leftrightarrow 2$ on a Volt-meter, see Figs. 5 and 6. The experimental evidence [13] in Fig. 6 indicates that in this case

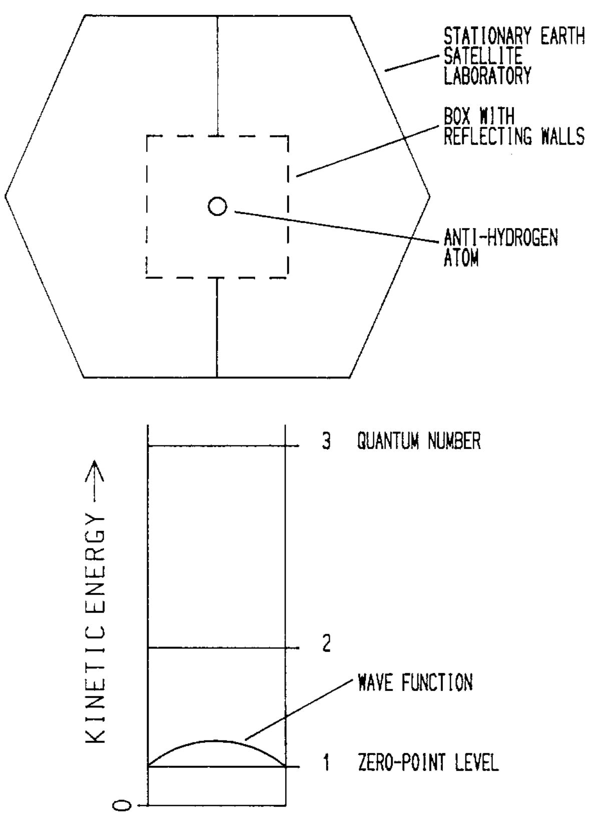

Fig. 2. Individual antihydrogen atom floating at rest in the inertial frame of a stationary earth satellite laboratory [3]. For a box size of $\frac{1}{2}$ mm the zero-point energy corresponds to a temperature of $\approx 10^{-11}$ K, and the non-material walls of the box could comfortably be formed by a magnetic trap employing fields no larger than 100 μGauss.

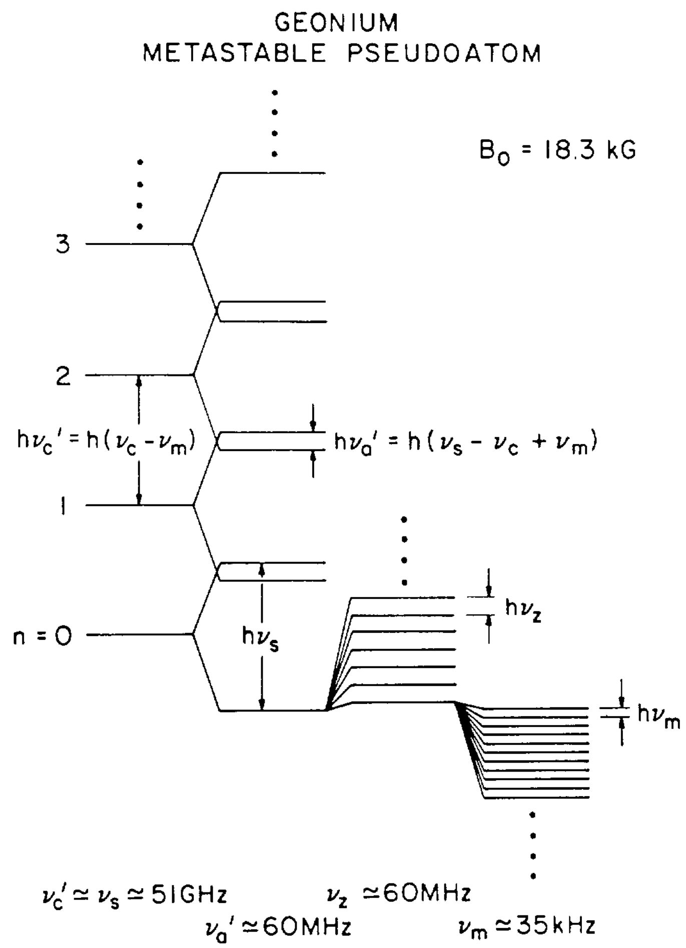

Fig. 4. Energy levels of geonium. Parameter values for an early experiment are shown. They were chosen to make $\nu_s - \nu_c \approx \nu_z$ for ease of creation of an effective magnetic r.f. field at $\nu_s - \nu_c$ by shaking the electron at that frequency in the auxiliary magnetic bottle primarily used for the Stern–Gerlach efect [16].

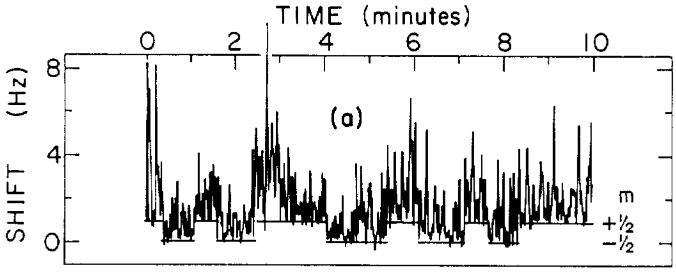

Fig. 5. Continuous Stern-Gerlach effect data for continuous two-photon excitation of spin flips and simultaneous observation of the spin state. This excitation was provided by a coherent r.f. field at $\nu_s - \nu_c$ and thermal radiation at ν_c. The abrupt jumps in the lower border of the noise band at random intervals signal the spin flips $m = +\frac{1}{2} \leftrightarrow -\frac{1}{2}$ [18].

the electron spends $\approx 90\%$ of its time in the lowest cyclotron energy level, $n = 0$. Total zero-point confinement $(mnkq) = (-\frac{1}{2}000)$ appears possible [21], when *cavity-enhanced* ν_c side band cooling is used. See the discussion of the cooling limit in Section 9.

3. Sideband excitation

Periodic motions of emitters or absorbers in a trap, due to the Doppler or related effects, produce sidebands [1] of their internal frequencies higher and lower by a trap frequency, as discussed by Dehmelt and Walls in 1968 [22]. In the same paper these authors also proposed to produce efficient spin relaxation for electrons in a Penning trap via assisted Majorana spin flops due to the cyclotron motion in an inhomogeneous r.f. magnetic field of frequency $\nu_s - \nu_c$, the lower side band of the spin frequency. Simultaneously Walls, in his 1970 doctoral thesis work at the University of Washington, attempted to make use of this relaxation effect: in a cold gas of trapped electrons, whose spin resonance was saturated, heat from the hot spin system would be transfered to the cold cyclotron motion, the ensuing increase in the temperature of the electron gas signaling the spin resonance condition. This was an early proposal to produce side band *heating* (here of the cyclotron motion at ω_c). The opposite process, side band *cooling*, was proposed by Wineland and Dehmelt in 1975 [23], after they had searched for such heating and cooling effects in electron clouds on and off since 1971. Side band cooling was first demonstrated (in the r.f. region)

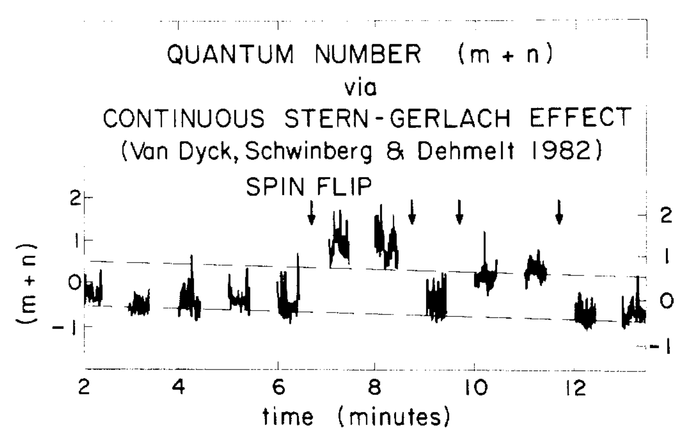

Fig. 6. Continuous Stern–Gerlach effect data as observed by alternating periods of perturbation and of observation of the spin state [13, 16]. When the excitation at $\nu_s - \nu_c$ is on, the axial frequency measurement is off, and vice versa.

by Van Dyck *et al.* [15, 16] in 1976. To explain this process in more detail, we consider an atom oscillating at ω along the x-direction and irradiated by a wave originating in a fixed source and propagating in the positive x-direction, see Fig. 7. Due to the Doppler effect, the sharp frequency of the source radiation then develops at least two side bands, spaced at ω, when viewed from the rest-frame of the atom. When the radiation is tuned so, that the upper side falls on the atomic resonance Ω, the atom is excited and in its co-moving frame re-radiates the frequency Ω. Observers in the laboratory frame, again due to the Doppler effect, will see the emission at Ω, but also two side bands, whose intensity depends on the observer location. The average re-emitted frequency of the re-emission will be $\approx \Omega$. Since the energy of an incoming photon is $\hbar(\Omega - \omega)$ in the lab frame, while, on the average, that of a re-emitted photon is $\approx \hbar\Omega$, the balance $\hbar\omega$ has to come from the vibrational motion, which is thereby cooled. By the use of such techniques Van Dyck *et al.* [3] were able to announce on 15 September 1984: "Here, right now, in the center of our Penning trap resides positron Priscilla in a little cylinder 30 μm in diameter and 60 μm long, and has been executing simple spontaneous ballet routines for the last 3 months!" (There can be little doubt about the identity of Priscilla during this period, since she never had the chance of trading places with a passing twin.)

4. Outstanding result: new value for electron radius

The close confinement of the electron described above was an important ingredient in our experiments [13, 15–18] on its g-factor. Following Gardner and Purcell [24], the g-factor is defined as $g = 2\nu_s/\nu_c$, ν_s and ν_c denoting spin and cyclotron frequencies respectively. Our experiments allow us to address the fundamental question: Is the electron a point? The vanishing radius, $R_{\mathrm{Dirac}} = 0$, of the ideal Dirac particle may be viewed as an unphysical mathematical convenience. The actual physical electron is assumed to be merely too small to measure with today's techniques. The physical electron of charge e is likely to be a *near*-Dirac particle, similar to the proton. For the proton, Hofstadter in 1956 measured an rms

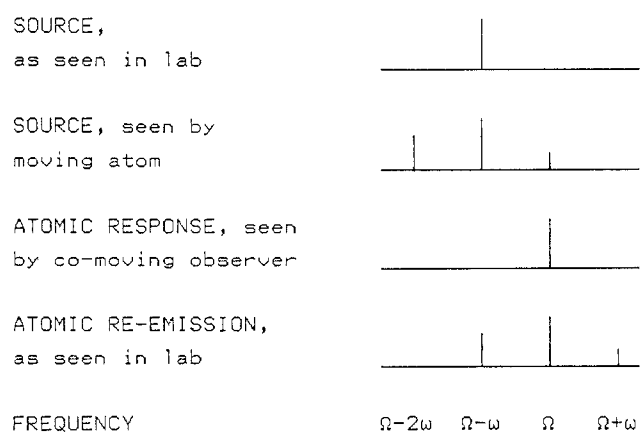

Fig. 7. Side band cooling. The vibrational motion at ω of the center of mass of a trapped atom is cooled by a plane wave tuned to the lower Doppler side band at $\Omega - \omega$ of an internal resonance at Ω. In the laboratory frame the source emits photons of energy $\hbar(\Omega - \omega)$, which the moving atoms absorbs, and then re-emits with average energy $\hbar\Omega$. The balance $\hbar\omega$ has to come from the vibrational motion which is thereby cooled.

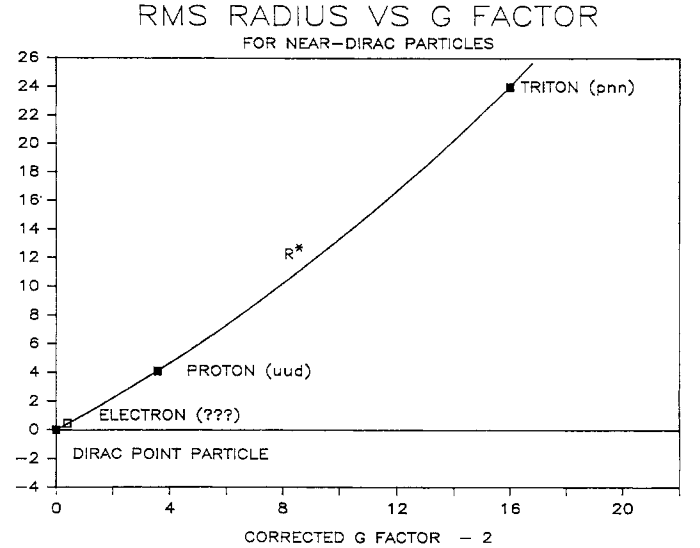

Fig. 8. Normalized RMS radius $R^* = R/\lambda\!\!\!^{-}_C$ vs. corrected g-factor minus 2 for near-Dirac particles [3]. A parabola has been fitted to the data points. Recent theories conjecture that the electron, similar to proton and triton, is composed of three smaller fermions. The data point at the origin represents a Dirac point particle of finite arbitrary charge and mass.

radius [25, 26]

$$R = 8.6 \times 10^{-14}\,\text{cm}.$$

This may be compared to the radius of its quasi-circular Schrödinger Zitter-Bewegung. The radius [27, 28] of this spontaneous "orbital" motion is $\lambda\!\!\!^{-}_C$, the Compton wavelength. The large value of the plausible deviation measure

$$(R - R_{\text{Dirac}})/\lambda\!\!\!^{-}_C = R/\lambda\!\!\!^{-}_C \approx 4$$

shows, that the proton, the closest approximation of a Dirac particle after electron and muon, is not a very close one. Perhaps it is then not surprising, that its g-factor is not close to the Dirac value 2 either, and that another dimensionless deviation measure also has a large value, namely

$$g - g_{\text{Dirac}} \approx 3.6.$$

The value $g \approx 5$ was measured by Stern in 1933 in another one of the great early experiments [29, 30] of elementary particle physics. Prior to it everybody "knew", that the proton was a Dirac particle with $g = g_{\text{Dirac}} = 2$, and $R = R_{\text{Dirac}} = 0$. Forming the Dirac-deviation ratio

$$\rho_D \equiv [(R - R_{\text{Dirac}})/\lambda\!\!\!^{-}_C]/(g - g_{\text{Dirac}}),$$

one finds for the proton:

$$\rho_D \approx 1.$$

This appears impressive to a Pythagorean, and encourages the conjecture $\rho_D \approx 1$ for *other* near-Dirac particles too. Figure 8, presenting an experimental data plot of the normalized rms radius $R/\lambda\!\!\!^{-}_C$ vs. g for the few known (composite) near-Dirac particles, appears to corroborate this conjecture. It is tempting to view the electron as formed by very tightly binding together three smaller and much heavier new fermions [31], whose liberation would require currently unavailable energies. However, extrapolation then almost forces one to postulate a progression of new, smaller and smaller, and less and less imperfect Dirac particles with ever increasing masses. This progression stretches up to "the" elementary particle, a member of the lone, "cosmon/anticosmon" pair,

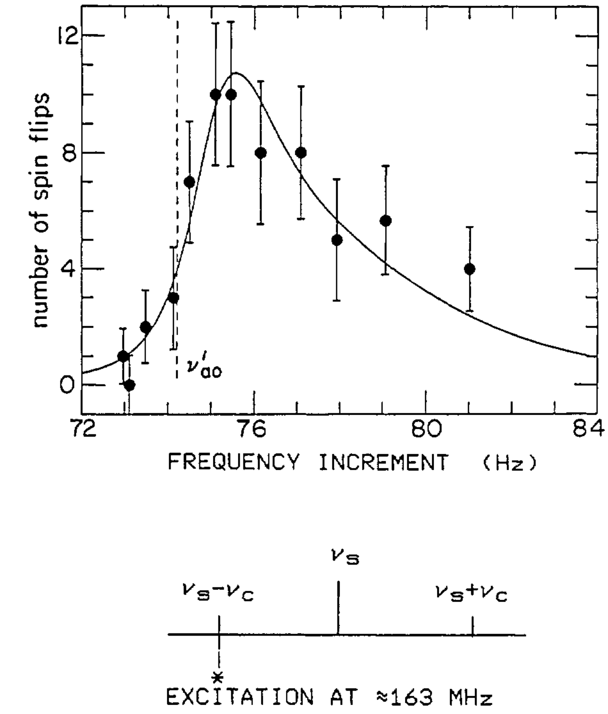

Fig. 9. Spin resonance at $\nu_s \approx 141$ GHz [32]. Each point represents the total of spin flips counted in 25 excitation/observation cycles. Actually excited is a side band of the spin resonance at $\nu_s - \nu_c \approx 163$ MHz produced by the cyclotron motion at ν_c through an inhomogeneous r.f. field at $\nu_s - \nu_c$ [22], see lower part of figure. Note steep left slope of ≈ 2 Hz width!

into which the metastable vacuum dissociated in a random quantum jump, the big bang. A model, in which these massive very shortlived particles are extremely tightly bound together would preserve the requirement of vanishing total relativistic energy. Their subsequent disintegration would then form the universe. The "cosmon/anticosmon" pair or "cosmonium" atom introduced here is merely a modernized version of Lemaître's "primeval atom".

For the electron, with $\lambda\!\!\!^{-}_C(e) \approx 4 \times 10^{-11}$ cm, and after applying QED corrections to g_{Dirac}, one obtains, assuming $\rho_D \approx 1$,

$$R_g \approx 4 \times 10^{-11}\,|g^{\text{exp}} - g^{\text{qed}}|\,\text{cm} < 10^{-20}\,\text{cm}.$$

This is $10^4 \times$ smaller than the accepted value, and agrees with the analysis of Brodsky and Drell [31]. Here we have used our experimental value [32], see Fig. 9,

$$\tfrac{1}{2}g^{\text{exp}} = 1.001\,159\,652\,188(4),$$

which is about 1000 times more accurate than the best previous work in another laboratory, compare [17]. The most recent result of the heroic calculations of Kinoshita [33] is

$$\tfrac{1}{2}g^{\text{qed}} = 1.001\,159\,652\,263(22)(104).$$

The two error brackets refer separately to the numerical QED calculation and α^{exp}. Accordingly, there is currently a premium on better experimental values for the fine structure constant α^{exp}, and even more accurate theoretical g^{qed} values.

5. Crucial ingredient: continuous Stern–Gerlach effect

In the classic, destructive Stern–Gerlach experiment on

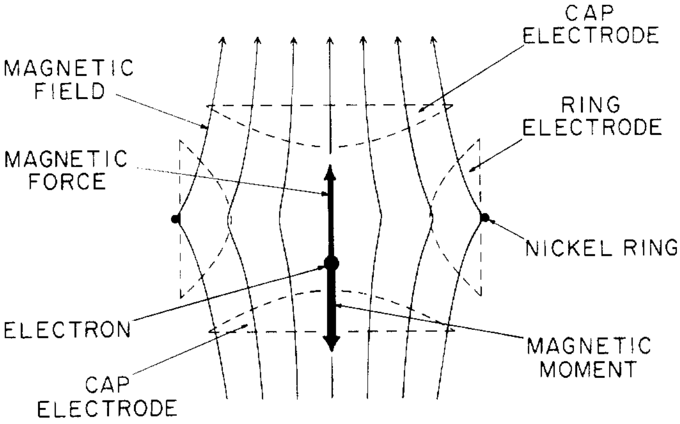

Fig. 10. Shaped magnetic field gradient for Continuous Stern–Gerlach effect. The gradient provides a very shallow supplementary spin-dependent parabolic monitoring potential, slightly shifting the axial frequency ν_z. The gradient is created by a ferromagnetic nickel wire wound around the ring electrode, which slightly deforms the principal ≈ 5 Tesla field [2].

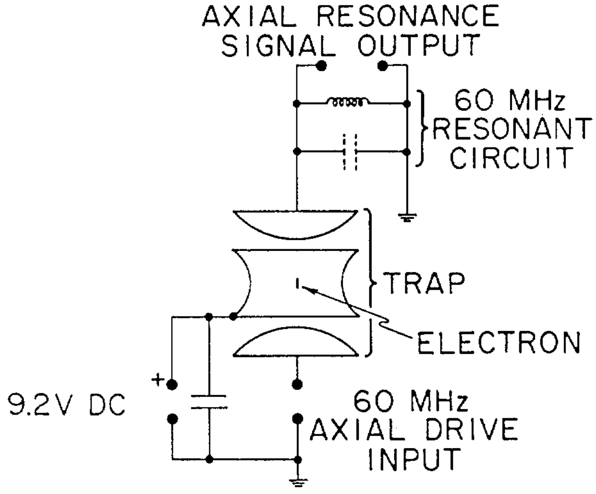

Fig. 11. Trajectory sensor for continuous Stern–Gerlach effect. The spin-dependent parameter of the classical trajectory observed by this axial resonance detector is the frequency of the axial motion ν_z.

a beam of silver atoms, the atoms were allowed to bury themselves in a spot condensate on a glass plate in order to cause them to reveal the spin direction they had in their former lives, before their demise as free particles. By contrast, in our continuous version, the individual localized electron only scatters a large number of soft r.f. photons, and emerges from the gentle measurement process as a free particle in the spin state thus determined. The principal hypothesis of quantum mechanics (see, e.g., Ref. [34]) states, that a measurement of an observable can only yield one of the possible eigenvalues of that observable, and throws the system into the corresponding eigenstate of that observable. If these eigenstates are also eigenstates of the energy and therefore stationary, and the same measurement is repeated at a later time, the result must be the same as that found originally. Our experiments appear to represent one of the few instances, if not the only one, in which a measurement on the same individual atomic particle has been repeated, and the latter part of the hypothesis has been actually tested directly. (The recently demonstrated shelved electron amplifier, described in Section 9, is similar but much less gentle, since it relies on internal atomic excitations for state monitoring).

Following Pauli [34], the apparatus for the continuous Stern–Gerlach effect [17, 35, 36], as that for the classical one, has two principal components. One is a shaped magnetic field gradient, see Fig. 10, and the other one is an orbit sensor, Fig. 11. The main ≈ 5 Tesla magnetic field is supplemented by a weak magnetic bottle, similar to that in Lawrence's cyclotron [9], which provides the gradient. This bottle contributes minutely to the axial trapping in a spin- and cyclotron orbit-dependent way, thus modifying the axial oscillation frequency of the electron to

$$\nu_z = \nu_{z0} + (m + n + \tfrac{1}{2})\delta,$$

where $\nu_{z0} \approx 60$ MHz is the axial frequency in the absence of the magnetic bottle, and typically $\delta \approx 1$ Hz. When the geonium atom is only thermally excited *and suitably observed*, the electron is seen to jump [15] frequently between the cyclotron levels n, but almost never between the spin levels m. For an in-cavity cyclotron life time τ_{cc}, the average uninterrupted dwell time in the $n = 0$ ground state is found [20] to be

$$t_0 = \tau_{cc}[\exp(h\nu_c/kT) - 1].$$

Also, for $h\nu_c \gg kT$ the fraction of total time spent out of $n = 0$ is $f \approx \exp(-h\nu_c/kT) \ll 1$. Cooling to 4 K, makes the cyclotron quantum number $n = 0$ for random intervals of average length $t_0 \approx 10\tau_{cc} \approx 10$ s, and $f \approx 0.1$. This greatly simplifies the procedure. Still, in order to identify the spin states $m = +\frac{1}{2}, -\frac{1}{2}$, obviously a very sharp axial resonance is required, whose frequency ν_z can be measured to $\ll 1$ Hz. The frequency meter used for this purpose is our new version of "orbit sensor" mentioned above, and it replaces the glass plate of the classic experiment. Like the separation of the silver deposits, measuring $\nu_z(m = +\frac{1}{2}) - \nu_z(m = -\frac{1}{2}) = \delta$ yields a rough value of the magnetic moment μ_s, not only the dimensionless ratio g!

Our continuous Stern–Gerlach effect may be generalized. Given a main trapping well of depth D_z^e, width $2Z_0$, and an axial oscillation frequency ν_z, any added monitoring well of the same width, and depth D_z^m, increases ν_z by

$$\delta\nu_z = \tfrac{1}{2}\nu_z(D_z^m/D_z^e).$$

Using in conjunction with a Penning trap a magnetic monitoring bottle with a maximum bottle field H_{max}^b produces an additional well depth

$$D_z^m = \mu_z(mnkq)H_{max}^b,$$

and a shift $\delta\nu_z$ reflecting the quantum numbers of the geonium state of total magnetic moment $\mu_z(mnkq)$. Analogously, an auxiliary laser trap, similar to one recently demonstrated by Chu *et al.* [37], would yield a well depth of about

$$D_z^m = \alpha(nJLM)\langle E^2(z)\rangle_{max},$$

Table I. *Generalized continuous Stern–Gerlach effect for Mono-Ion oscillator (MIO)*

System	D_z^m	D_z^e	$2Z_0$	ν_z	δ
Geonium + mag. bottle	0.1 μeV	5 eV	10 mm	60 MHz	1.2 Hz
Ba^+ MIO	–	1.2 eV	1 mm	1 MHz	–
Ba^+ MIO + laser trap	1 μeV	120 μeV	10 μm	1 MHz	8 kHz!

the laser electric field average to be taken over an oscillation period of the laser. Here $\delta\nu_z$ would give information on the quantum numbers of an atomic ion of polarizability $\alpha(nJLM)$ confined in, say, a Paul r.f. trap. Table I compares δ-values for geonium [17] and trapped Ba^+ [4]. Note the huge $\delta = 2[\nu_z(E \text{ on}) - \nu_z(E \text{ off})]$ value for small oscillations of the Ba^+ ion!

6. Electron–cavity interaction

In order to make the spontaneous emission at ν_z by the oscillating electron in Fig. 11 detectable, which in free space would be vanishingly small, it is 10^8-fold enhanced by surrounding the electron with a resonant "cavity", formed by the cap electrodes and a high-Q coil. Thus, when a calibrated drive excites the axial oscillation, its eigenfrequency ν_z may be precisely measured, by picking up the enhanced emission with a radio receiver, and tuning the calibrated drive to the vanishing point of the dispersion part of the signal. Cavity enhancement of emission, discussed for atoms by Purcell in 1946 [38], is not so strange. After all, considerable power has been extracted from electron cyclotron oscillations this way in the split-anode magnetron since the 1920's [39].

Townes and Schalow [40] in 1955 also discussed the opposite effect, cavity suppression of emission by tuning *between* two cavity eigenfrequencies [19, 41]. Thus, for an elastically bound electron surrounded by a super-conducting sphere of radius $a \gg \lambda$, one should expect in general almost total suppression of spontaneous emission as long as the electron frequency does not coincide with a cavity eigenfrequency, as there is no way for the radiation to get out. At the same time the cavity does in general produce a shift of the resonance frequency of the electron,

$$\delta_c/\omega_e = -(r_e/3a)F(Y),$$

with $Y = \pi X$, $X = 2a/\lambda = a\omega_e/\pi c$ [42, 43], Fig. 12. While the cavity shift is very undesirable, we note, however, that $F(Y)$ and the shift vanish for $X \approx 1\frac{1}{2}, 2\frac{1}{2}, \ldots$. This vanishing of the shift *between* cavity eigenfrequencies is an important general feature of all cavities, as pointed out before [41]. At the zero-shift tuning points the wave emitted by the electron, after reflection by the spherical cavity wall, returns with such a phase, that the force exerted by its electric field on the electron is in phase with the electron velocity. Then the reflected wave is completely re-absorbed by the electron, thereby cancelling the radiation damping. For this phasing of the field there is no modification of the force constant of the bound electron due to the wave field and therefore no shift of the electron frequency, while the natural line width is almost completely suppressed.

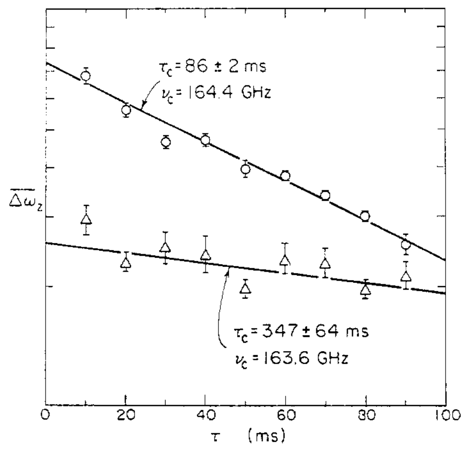

Fig. 13. Suppression of spontaneous emission of cyclotron radiation [45]. Plotted is the slow decrease of the electron mass after termination of a modest cyclotron excitation.

As a beginning, for the important cyclotron motion an in-cavity damping time of ≈ 1 s, 10-fold larger than the vacuum value, has been demonstrated by Gabrielse *et al.* [13, 44, 45] at the University of Washington, see Fig. 13. The dwell time in our systems is practically unlimited, allowing full exploitation of the expected 10-fold reduction of the natural line width. Large decreases of the emission *rate* have been reported also for later beam experiments conducted at higher frequencies [46–48]. However, only in one of them seems the dwell time to have been long enough to make this useful. Furthermore, all beam work presumably was affected by sizeable cavity-induced frequency shifts.

7. Fine structure of the cyclotron resonance

Eventual replacement of the continuous Stern–Gerlach effect by the Kaufmann-Einstein effect was proposed in 1974 [49].

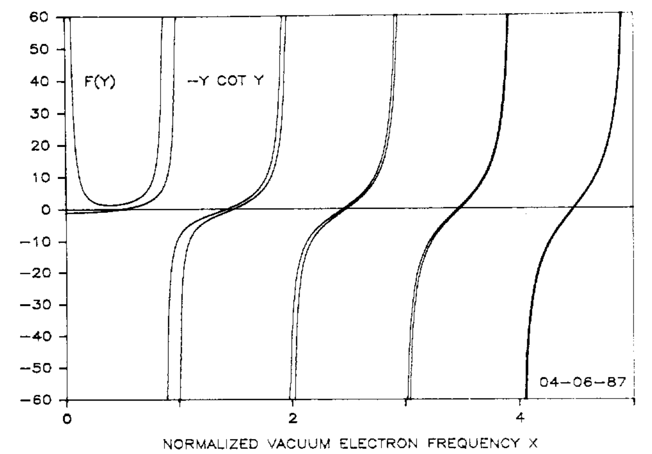

Fig. 12. Frequency shift function $F(Y)$ for spherical cavity of radius a, $X \equiv 2a/\lambda$, $Y \equiv \pi X$, from Ref. [42]. Note occurrence of shift zeros *between* eigenfrequencies of the cavity!

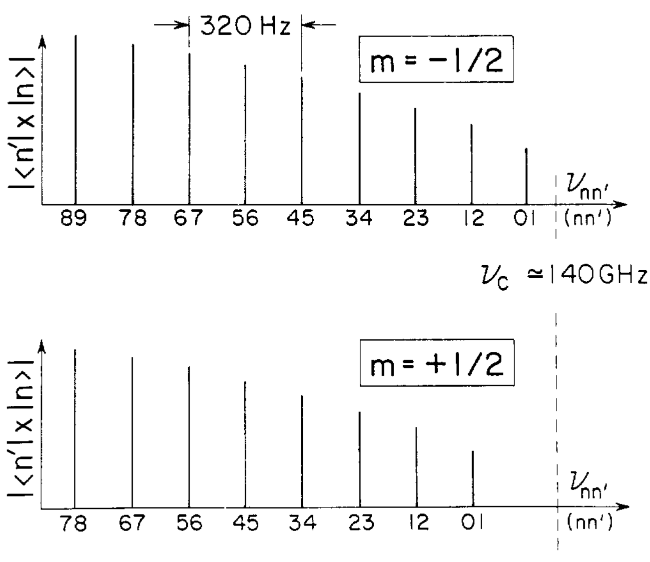

Fig. 14. Relativistic fine structure of geonium cyclotron resonance spectrum [2]. Note the isolated ν_{01} component for spin down, which flags the $m = -\frac{1}{2}$ state.

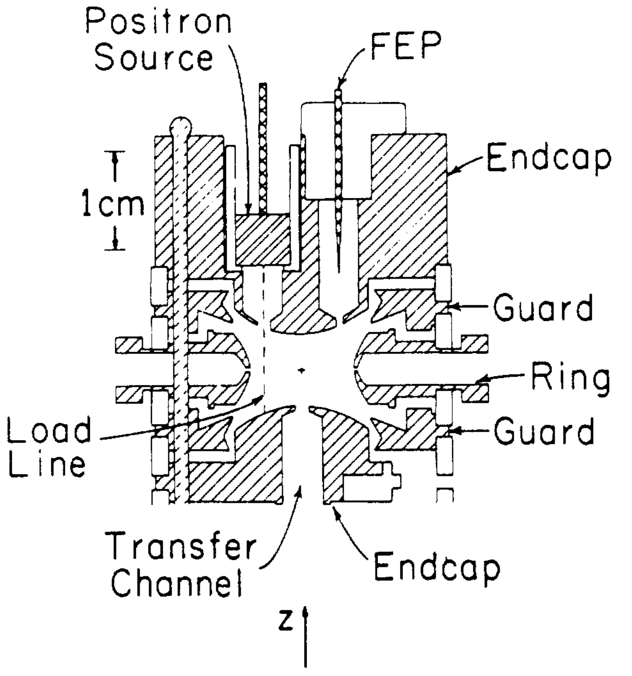

Fig. 15. Auxiliary trap used to catch and store β^+ particles from built-in < 1 m Curie source for later transfer into principal trap used for geonium spectroscopy [54].

These authors quoted a Landau Level dependent relativistic shift in the axial frequency $\nu_z = 60\,\mathrm{MHz}$ of value

$$\delta\nu_z = -(m + n + \tfrac{1}{2})\nu_z h\nu_c/2mc^2.$$

For $\nu_c = 140\,\mathrm{GHz}$ this yields a shift of $\approx 0.034\,\mathrm{Hz}$ per Landau level. Accordingly, with our present shift monitor a cyclotron excitation to only $n = 3$ should be barely detectable.

Employing the relativistic cyclotron fine structure [17], see Fig. 14, as spin monitor, and use of the lone electron itself as powerful amplifier of its own very sharp $n = 0 \rightarrow 1$ transition was suggested in 1980 [2, 50]. Along these lines it is difficult to see, how a simple quasi-thermal excitation scheme [51] making use of a hot, 8 kHz wide nearly rectangular noise band, even in the presence of residual broadening of the fine structure components [50] and/or of the microwave source to $\approx 50\,\mathrm{Hz}$, should not produce a *detectable, frequency selective* "heating" of the cyclotron motion to $\langle n \rangle \approx 30$ in $\approx 2\,\mathrm{s}$ with apparatus largely in place.

Beginning in 1975 [52], modest progress was made with a couple of preliminary exercises based on other schemes [2], the latest one succeeding in a classical synchro-cyclotron operation of the geonium atom [53] of limited frequency selectivity. A new, non-QED, value for the fine structure constant α may be another future fruit of these continuing efforts [3].

8. Geonium extensions to antimatter

The first experiments to trap antimatter in a Penning trap were carried out in 1981 [54], see Fig. 15. By first moderating and decelerating to millivolt axial energies, and then eccentrically injecting positrons from a weak < 1 milliCuri positron emitter built into the vacuum envelope of the trap tube, Schwinberg *et al.* [54] succeeded in continuously trapping small numbers of positrons. In this process a positron of very low axial, but $\approx 100\,\mathrm{keV}$ cyclotron energy, after entry into the auxiliary "reservoir" trap, was made to complete one full magnetron orbit. During this interval enough axial energy was extracted by resonant damping or enhanced spontaneous emission, see above, that it became permanently trapped. After a few seconds the positron had lost all excess axial and cyclotron energy in this way, became thermalized, and could be centered by side band cooling of the magnetron motion on the axial resonance. From the reservoir trap, when needed, a positron could be transferred into the regular trap used for our geonium spectroscopy experiments, and studied in exactly the same fashion as an electron.

Continuing work along these lines has very recently [32] yielded a test of the CPT theorem to 2×10^{-12} for the *charged* e^+/e^- particle/antiparticle pair of leptons. Only experiments on the neutral K-meson pair yield a more rigorous test of this symmetry. Geonium type experiments were proposed for the antiproton in 1973 [11], and again in more detail in 1979 [55]. In 1986, Gabrielse *et al.* succeeded in catching a few hundred antiprotons from the Low Energy Antiproton Ring at CERN in a rough Penning trap. Since earlier Van Dyck *et al.* [56] had demonstrated the continuous r.f. detection of an individual proton in a Penning trap, the way is now open for a new high-precision CPT test also on the proton/antiproton pair of charged baryons, as discussed by Gabrielse in these Proceedings.

9. Extension to optical spectroscopy

In 1973 in Seattle I proposed the Tl^+ mono-ion oscillator [57] for $\Delta\nu/\nu < 10^{-14}$ ultrahigh-resolution optical spectroscopy. This device made use of a different trap, the Paul r.f. trap [1, 6], which produces a true 3-D well potential well, marred only by the tiniest r.f. heating. In preparation for this ambitious goal, I proposed, together with Toschek in 1974 [58] in Heidelberg, to make an individual Ba^+ ion visible by illuminating it with laser light in a similar apparatus. In 1979 Neuhauser *et al.* succeeded in Heidelberg to see and photograph such an ion [4]. These experiments made use of laser side band cooling [23], which in a 1976 ONR research proposal of limited distribution and a later publications [59, 60] I had shown to be capable of zero-point confinement in the case of Tl^+. The minimum average value of the vibrational

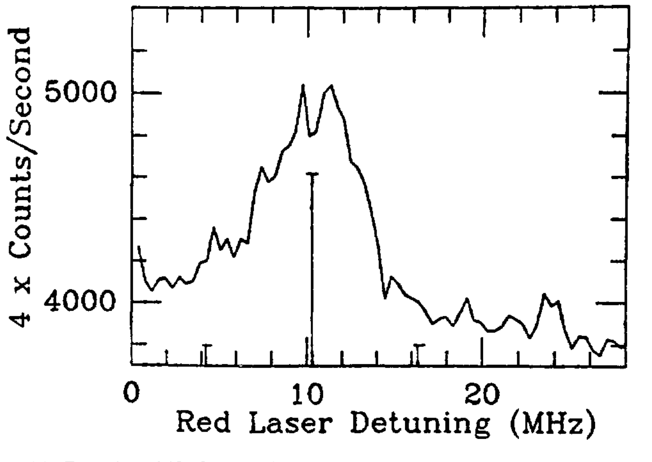

Fig. 16. Doppler shift free optical spectrum of individual Barium ion at 2.06 μm [61]. The absence of side bands at the 6 MHz oscillation frequency, indicates unambiguously, that the oscillation in the trap has an amplitude much smaller than the optical wave length.

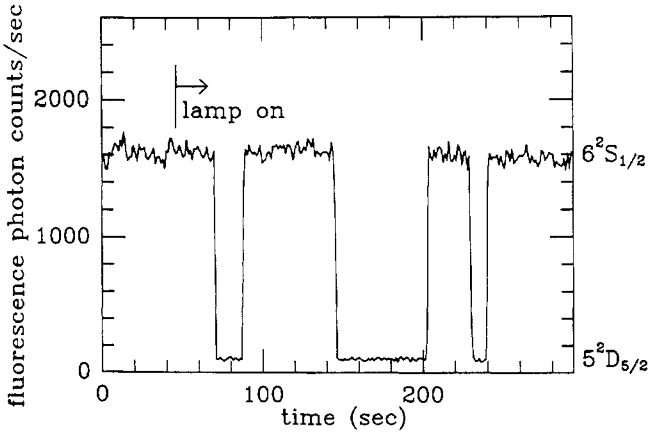

Fig. 17. Demonstration of "shelved (optical) electron amplifier" and quantum jumps. The strong, laser-excited resonance fluorescence is turned off for about 30 s by a jump of the electron into the $D_{5/2}$ shelf level, causing the loss of $\approx 10^8$ fluorescence photons [5]. The jump is initiated by the atom absorbing a single photon of lamp radiation!

quantum number attainable by this method is

$$\langle v \rangle_{\min} \approx (3/16)(\gamma/\omega_v)^2 \ll 1,\ \omega_v \gg \gamma.$$

An average value $\langle v \rangle_{\min} \ll 1$ implies that, following a cooling cycle, the vibrational quantum number will almost always have the value 0. A single strategically oriented laser beam suffices for three-dimensional cooling [23, 57]. A number of other workers have later studied laser cooling from different points of view and confirmed the essential correctness of the above result. No zero-point confinement of an atomic ion has been reported to date. However, a 2.07 μm Ba^+ transition has been resolved by Janik *et al.* [61] well enough to distinguish any Doppler side bands spaced at 6 MHz, see Fig. 16. As is routine in NMR of gaseous samples, in which the molecules are rapidly moving but localized to a region $\ll \lambda/2\pi$, no Doppler side bands were observed in our experiments. In conjunction with the only modest signal/noise ratio attained, this translates to a localization of the Barium ion in the trap of

$$\langle x^2 \rangle \approx \langle y^2 \rangle \approx \langle z^2 \rangle < (120\,\text{nm})^2,$$

and confirmed earlier claims [4, 59]. More recent similar work by others has demonstrated even better localization.

Mono-ion high-resolution spectroscopy is made possible by the $10^6\times$ shelved electron amplifier [62], which was recently demonstrated at the University of Washington [5] and confirmed elsewhere. The use of this scheme, both at the University of Washington and in other laboratories, has also yielded a very clear and unambiguous demonstration of quantum jumps, Fig. 17, after a quite respectable demonstration of jumps between spin states had been achieved in the early geonium work, see Fig. 5. Both the Seattle and Hamburg versions of the "shelving" amplifier employ Ba^+. Its terms are shown in Fig. 18, which makes it clear that once the atom has somehow been promoted into the metastable $D_{5/2}$ state of ≈ 30 s lifetime, it will be incapable of the strong laser-excited fluorescence at 493 nm, which makes it visible. In Fig. 17 two-step excitation into $D_{5/2}$ was achieved by turning on an auxiliary spectral lamp.

This is obviously a very effective monitor of the forbidden $S_{1/2} \to D_{3/2}$ transition at 1.76 μm, which exhibits an admirable sharpness, 5.3 mHz. Appropriate pulsing schemes should allow approaching this width, and a suitable commercial

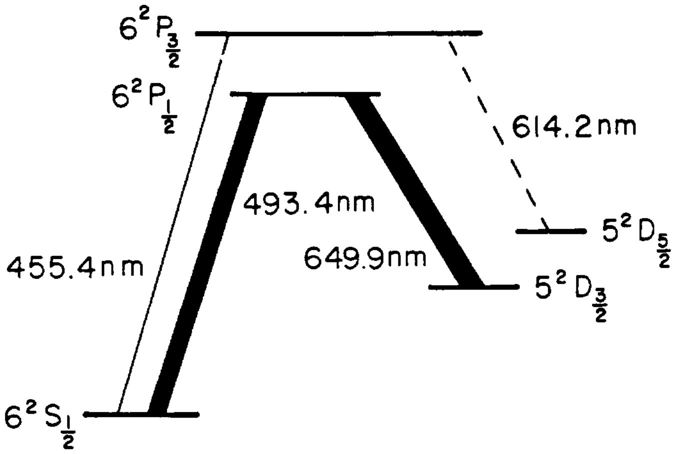

Fig. 18. Energy levels of Ba^+. The life time of the metastable $D_{5/2}$ "shelf" level is ≈ 30 s. The 455.4 nm radiation is provided by a spectral lamp [55].

laser has just become available. Another promising candidate is a stored ion laser, in which in distinction from current lasers, and as in the H-maser, the oscillation frequency is determined by the atoms and not by the cavity [63], as proposed by Fortson *et al.* in 1966.

Forbidden transitions between two states, both having vanishing total angular momentum, $J = 0$, but of course $I = F \neq 0$, are of special interest, because they exhibit minimal coupling of the electronic electric quadrupole moment to residual fields in the trap. Good examples are the $^1S_0 \to {}^3P_0$ transitions in Tl^+, In^+ or analogous ions. Use of this type of transition, in combination with the shelving amplifier described above, may make an optical frequency standard/clock with a resolution and 1000-day reproducibility 10^{-18} possible [64]. Such a level of reproducibility would be highly desirable in a search for a conceivable time-variation of fundamental constants paralleling the Hubble expansion of the universe. The resolution envisioned may also be sufficient for a meaningful experimental re-examination of the notion of "identical" clocks. The total identity of two bodies appears to require their location in the same spot. As the identity of ion clocks A and B, both employing the same species of ion, can only be guaranteed by confining them in different traps, one appears to have run into a paradox here. With other words, no two clocks can be completely identical.

10. Future extensions to exotic species

Various systems of interest may be synthesized [3] and retained in a Paul r.f. trap soon. I mention hydrogenic U^{91+} stabilized in a circular Rydberg orbit by a superconducting spherical cavity. Further on, some physicists may do spectroscopy and free fall experiments, see Fig. 2, on an antihydrogen atom $\bar{H}$, synthesized from a positron-antiproton plasma in a r.f. trap. Currently most promising for atomic antimatter physics is the antiparticle of the molecular hydrogen ion H_2^+, with rich r.f. and infrared spectra. In a Paul r.f. trap, loaded with a plasma of many LCR-cooled positrons and a few antiprotons, synthesis and confinement of it and possibly even a singly charged polymolecular antihydrogen cluster seem feasible today. The forbidden microwave and infrared spectra of an individual diatomic molecular ion of antihydrogen might then be measured to a revolutionary resolution, and be compared to those of the normal molecular ion. What is needed here is a mechanism for analyzing, in gentle fashion, the quantum state of the ion confined in a Paul r.f. trap before and after the, say, rotational transition under study. Just as for geonium, the preferred channel of communication with the ion would be via its axial motion at $\nu_z \approx 10\,\text{MHz}$. Here the novel generalized continuous Stern–Gerlach effect, employing an optical monitoring trap produced by a focussed laser beam, see Section 5, might be effective. This would solve the analyzing problem for this fundamental molecule which is also interesting as testing ground for conceivable new long-range proton–proton forces.

Future trapping of a now available antideuteron, and anti-helium 3, the latter both as nucleus and singly charged ion with optical and microwave spectra, appears worthwhile also.

Acknowledgements

I enjoyed conversations with James Bardeen, and Robert W. Williams. I thank Frederick Kaempffer and Richard Mittleman for comments, and Diana Dundore for reading the manuscript and suggesting improvements. The work was carried out under the auspices of the U.S. National Science Foundation.

References

1. Dehmelt, Hans, Advances in Laser Spectroscopy (Edited by F. T. Arecchi, F. S. Strumia, and H. Walther), Plenum, New York (1983).
2. Dehmelt, H., Annals de Physique (Paris) **10**, 777 (1985).
3. Dehmelt, H., Advances in Laser Science II (Edited by W. C. Stwally and M. Lapp), AIP Conference Proceedings No. 160 (1987).
4. Neuhauser, W., Hohenstatt, M., Toschek, P. E. and Dehmelt, H. G., Phys. Rev. **A22**, 1137 (1980).
5. Nagourney, W., Sandberg, J. and Dehmelt, H., Phys. Rev. Lett. **56**, 2797 (1986).
6. Dehmelt, Hans, in Adv. in At. and Mol. Phys. **3**, 53 (1967); **5**, 109 (1969).
7. Dehmelt, H., Phys. Rev. **103**, 1125 (1956).
8. Kingdon, K. H., Phys. Rev. **21**, 408 (1923).
9. Lawrence, E. O. and Livingston, M. S., Phys. Rev. **40**, 19 (1932).
10. Dehmelt, H., Bull. Am. Phys. Soc. **7**, 470 (1962).
11. Wineland, D., Ekstrom, P. and Dehmelt, H., Phys. Rev. Lett. **31**, 1279 (1973).
12. Hess, H. F., Kochanski, G. P., Doyle, J. M., Masuhara, N., Kleppner, D. and Greytak, T. J., Phys. Rev. Lett. **59**, 672 (1987).
13. Van Dyck, Jr., R. S., Schwinberg, P. B. and Dehmelt, H. G., in Atomic Physics 9 (Edited by R. S. Van Dyck and E. N. Fortson), p. 53, World Scientific Book Publishers, New York (1984).
14. Pierce, J. R., Theory and Design of Electron Beams, Section 4.41. Van Nostrand, New York (1949).
15. Van Dyck, Jr., R. S., Ekstrom, P. and Dehmelt, H., Nature **262**, 776 (1976).
16. Van Dyck, Jr., R. S., Schwinberg, P. B., and Dehmelt, H. G., in New Frontiers in High Energy Physics (Edited by B. Kursunoglu, A. Perlmutter, and L. Scott), Plenum, New York (1978).
17. Van Dyck, Jr., R. S., Schwinberg, P. B. and Dehmelt, H. G., Phys. Rev. **D34**, 722 (1986).
18. Van Dyck, Jr., R. S., Schwinberg, P. B. and Dehmelt, H. G., Phys. Rev. Lett. **38**, 310 (1977).
19. Dehmelt, H., Atomic Masses and Fundamental Constants 5 (Edited by J. H. Sanders and A. H. Wapstra), p. 504. Plenum, New York (1976).
20. Dehmelt, H., Ekstrom, P., Wineland, D. and Van Dyck, R., Bull. Am. Phys. Soc. **19**, 572 (1974).
21. Van Dyck, R. S., Schwinberg, P., Gabrielse, G. and Dehmelt, H., Bulletin of Magnetic Resonance **4**, 17 (1983).
22. Dehmelt, H. and Walls, F., Phys. Rev. Lett. **21**, 127 (1968).
23. Wineland, D. and Dehmelt, H., Bull. Am. Phys. Soc. **20**, 637 (1975).
24. Gardner, J. H. and Purcell, E. M., Phys. Rev. **83**, 996 (1951).
25. Chambers, E. E. and Hofstadter, R., Phys. Rev. **103**, 1454 (1956).
26. Simon, G. G., Schmitt, C., Borkowski, F. and Walther, V. H., Nucl. Phys. **A333**, 381 (1980).
27. Huang, K., Am. J. Phys. **20**, 479 (1952).
28. Dirac, P. A. M., The Principles of Quantum Mechanics, Paragraph 69, Oxford (1958).
29. Frisch, R. and Stern, O., Z. Physik **85**, 4 (1933).
30. Rabi, I. I., Kellogg, J. M. B. and Zacharias, J. R., Phys. Rev. **46**, 157 (1934).
31. Brodsky, S. J. and Drell, S. D., Phys. Rev. **D22**, 2236 (1980).
32. Van Dyck, Jr., R. S., Schwinberg, P. B. and Dehmelt, H. G., Phys. Rev. Lett. **59**, 26 1987.
33. Kinoshita, T., Proceedings of Conference on Precision Electromagnetic Measurements, Gaithersburg (1986).
34. Pauli, W., in Handbuch der Physik V/1 (Edited by S. Flügge), p. 64, Springer, Berlin (1958). I have relied only on the original german text.
35. Dehmelt, H. and Ekstrom, P., Bull. Am. Phys. Soc. **18**, 727 (1973).
36. Dehmelt, H., Proc. Natl. Acad. Sci. USA **83**, 2291 (1986).
37. Chu, S., Bjorkholm, J., Ashkin, A. and Cable, A., Phys. Rev. Lett. **57**, 314 (1986).
38. Purcell, E. M., Phys. Rev. **69**, 681 (1946).
39. Collins, G. B., Microwave Magnetrons, Ch. 1, McGraw-Hill, New York (1948) (Radiation Laboratory Series).
40. Townes, C. H. and Schalow, A. L., Microwave Spectroscopy, Section 13.1, McGraw-Hill, New York (1955).
41. Dehmelt, H., Proc. Natl. Acad. Sci. USA **81**, 8037 (1984); erratum **82**, 6366 (1985).
42. Dehmelt, H., Laser Spectroscopy VIII (Edited by S. Svanberg and W. Persson), Springer, New York (1987).
43. Brown, L. S., Helmerson, K. and Tan, J., Phys. Rev. **A34**, 2638 (1986).
44. Gabrielse, G., Van Dyck, R. S., Schwinberg, P. B. and Dehmelt, H. G., Bull. Am. Phys. Soc. **29** 926 (1984).
45. Gabrielse, G. and Dehmelt, H., Phys. Rev. Lett. **55**, 67 (1985).
46. Hulet, R. G., Hilfer, E. S. and Kleppner, D., Phys. Rev. Lett. **55**, 2137 (1985).
47. Jhe, W., Anderson, A., Hinds, E. A., Meschede, D., Moi, L. and Haroche, S., Phys. Rev. Lett. **58**, 666 (1987).
48. Heinzen, D. J., Childs, J. J., Thomas, J. E. and Feld, M. S., Phys. Rev. Lett. **58**, 1320 (1987).
49. Dehmelt, H., Ekstrom, P., Wineland, D. and Van Dyck, R., Bull. Am. Phys. Soc. **19**, 572 (1974).
50. Dehmelt, H., Atomic Physics 7 (Edited by D. Kleppner and F. M. Pipkin), Plenum, New York (1981).
51. Dehmelt, H. and Gabrielse, G., Bull. Am. Phys. Soc. **29**, 926 (1984).
52. Van Dyck, R., Wineland, D., Ekstrom, P. and Dehmelt, H., Appl. Phys. Lett. **28**, 446 (1976).
53. Gabrielse, G., Dehmelt, H., and Kells, W., Phys. Rev. Lett. **54**, 537 (1985).
54. Schwinberg, P. B., Van Dyck, Jr., R. S. and Dehmelt, H., Phys. Lett. **81A**, 119 (1981).
55. Dehmelt, H., Van Dyck, Jr., R. S., Schwinberg, P. B. and Gabrielse, G., Bull. Am. Phys. Soc. **24**, 757 (1979).
56. Van Dyck, Jr., R. S., Moore, F. L., Farnham, D. L. and Schwinberg, P. B., Bull. Am. Phys. Soc. **31**, 974 (1986).
57. Dehmelt, H., Bull. Am. Phys. Soc. **18**, 1521 (1973).
58. Dehmelt, H. and Toschek, P., Bull. Am. Phys. Soc. **20**, 61 (1975).
59. Neuhauser, W., Hohenstatt, M., Toschek, P. E. and Dehmelt, H. G., Phys. Rev. Lett. **41**, 233 (1978).
60. Dehmelt, H., Bull. Am. Phys. Soc. **24**, 634 (1979).
61. Janik, G., Nagourney, W. and Dehmelt, H., J. Opt. Soc. Am. **B 2**, 1251 (1985).
62. Dehmelt, H., Journal de Physique (Paris) **42**, Colloque C-8 Supplement, C8-299 (1981).
63. Fortson, E. N., Major, F. and Dehmelt, H., Phys. Rev. Lett. **16**, 221 (1966).
64. Dehmelt, H., IEEE Transactions on Instrumentation and Measurement, **IM-31**, 83 (1982).